POAC'13
Espoo, Finland

Proceedings of the 22nd International Conference on
Port and Ocean Engineering under Arctic Conditions
June 9-13, 2013
Espoo, Finland

STAMUKHA LOADING CASES FOR PIPELINES IN THE CASPIAN SEA

Ken Croasdale[1], Ken Been[2], Greg Crocker[3], Ralf Peek[4], Paul Verlaan [5]
[1]K.R. Croasdale & Associates (KRCA), Calgary, Canada
[2]Golder Associates, Halifax, Canada
[3] Ballicater Consulting, Kingston, Canada
[4]Shell Global Solutions, Rijswijk, The Netherlands
[5]North Caspian Production Operations Company, Atyrau, Kazakhstan

ABSTRACT

Ice surveys conducted in the Caspian Sea for the Kashagan Project during the period 2001 to 2010 have shown that stamukhi are frequent enough to create risks to pipelines. This paper reports on work aimed at bounding loads on the seafloor and pipelines due to the grounded ice keels of stamukhi. Gravity loading, as well as forces associated with ice sheet ride-up and subduction during stamukha formation, are considered. The ultimate bound on ice loading on the sea floor is the strength of the ice rubble. Typical pit sizes and depths in various soils due to the estimated ice pressures are calculated. Even if a pipeline is buried below the deepest predicted pits in ambient soils, weak backfill may lead to direct contact of the pipeline by the keel rubble of the stamukha.

INTRODUCTION

A stamukha is a grounded ice feature which often towers above the surrounding floating ice by several metres. Their presence in the Caspian Sea has been previously described in Nilsen and Verlaan, (2011). Large stamukhi are heavily grounded and usually have sufficient sliding resistance to resist the forces from the moving ice. Pits are often detected under heavily grounded stamukhi implying the occurrence of concentrated loads on the sea floor. In the Caspian Sea, stamukhi are frequent enough that pipelines in the region are at risk from a stamukha forming over them and creating loads.

EARLY APPROACHES TO PIT LOADS FROM STAMUKHI

Pits and stamukhi have been studied for the Kashagan development commencing in 2001 and continuing until 2010. In the early work, pit depths were measured under stamukhi by thermal drilling. The pit measurements were then treated statistically to develop pit depths with annual probabilities of 10^{-2} and 10^{-4} occurrence for a given pipeline (or as required by the codes).

Figure 1 shows typical thermal drill results on a selected drill line. This profile gives information on five relevant inputs to the problem; 1) the peak height of the stamukha along the line; 2) the porosity of the ice rubble making up the stamukha; 3) the water level; 4) pit depths relative to adjacent points along the sea floor and 5) the pit widths along the line.

The number of stamukhi in an area was initially determined from helicopter surveys. Later, helicopters equipped with laser mirror scanners were used to get above-water heights and shapes without the need for on-site drilling. Also later, pits were identified and measured using side-scan sonars and multi-beam echo sounders (MBES) from vessels immediately after break up. In some cases, locations with known stamukhi from winter surveys were targeted for MBES surveys.

Early results often gave pit depths greater than the scour depths at the same levels of probability. However, it is known that thermal drills can give conservative results because the hot water jet which melts through the ice can also jet into the upper layer of the sea floor giving the impression of a pit deeper than actual.

Regardless, the initial work led to criteria for loads on the sea floor and potentially on pipelines, based on either the gravity loads that could be concentrated on the pitted areas on the sea floor or the limiting strength of the ice rubble. These are now reviewed.

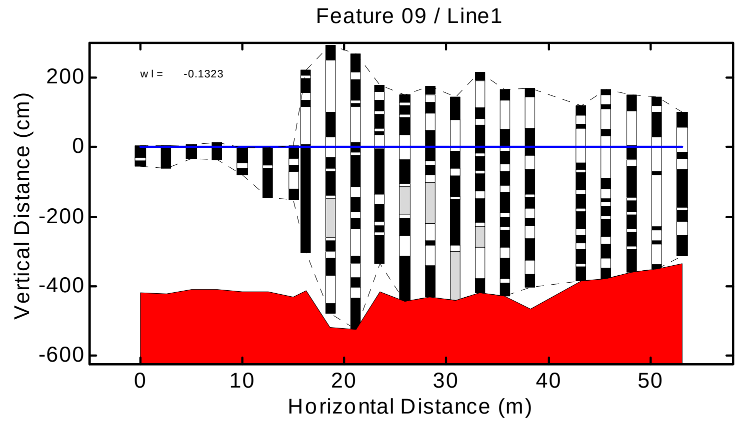

Figure1. Example of a thermal drill profile (Black –solid ice: White – void: Grey – slush: Red- seafloor showing pits)

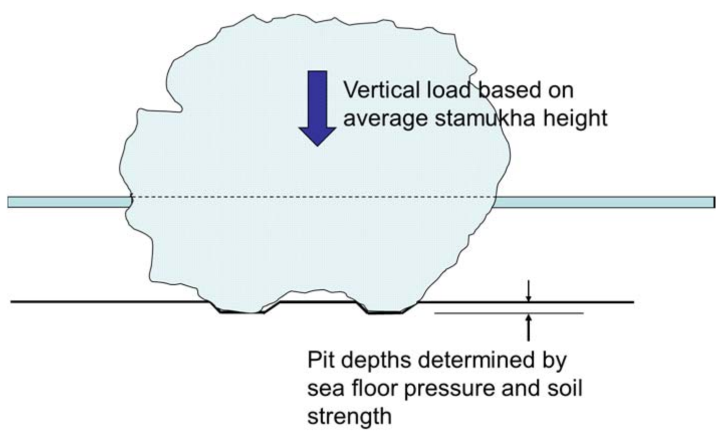

Figure 2. Schematic of stamukha forming pits

GRAVITY LOADING

A key interest in determining vertical forces under stamukhi is also to assess the potential for pits to be formed in a given soil. This is especially of interest when the backfill is weaker than the ambient soil and hence the pit depths based on pit statistics might have little relevance to design. Figure 2 shows how grounded stamukhi may transmit the out of balance hydrostatic loads into the sea floor to form pits. The ground pressures are based on average sail height, arching factors and pit sizes.

The key stamukha properties that determine gravity loads on the seabed are the sail height, ice density, porosity of the stamukha ice rubble and the number of grounding points.

The average pressure on the seabed under a stamukha (p_{ice}) can be calculated using the following equation:

$$P_{ice} = (1 - n_{ice}) \cdot (h \cdot \gamma_i + d \cdot (\gamma_i - \gamma_w)) \tag{1}$$

where, n_{ice} is the porosity of the ice and typically equal to 0.25; *h* is the average sail height of the stamukha; d is the water depth; γ_i is the unit weight of the ice, which is approximately equal to 8.8 kN/m^3;γ_w is the unit weight of the water, which is about 10.05 kN/m^3 for the North Caspian

Stamukha heights as great as 15m have been measured in the Caspian Sea. Based on this height and a typical Kashagan water depth of 4 m, a typical stamukha average grounding pressure under the high point of the stamukha is about 100 kPa. As shown later, this is sufficient to create pits in soft soils but not stiffer ones. However, two factors need to be considered in addition to this calculation. First, the maximum stamukha height occurs only at a point. Average observed stamukha heights tend to be in the range of 3 to 5m and the average distributed load would therefore be less than 100 kPa (about 20 – 30 kPa). Second, stamukha contact with the seabed is at discrete points and is not uniform. Stresses are therefore concentrated at contact points through arching within the ice rubble.

Based on early thermal drilling, an arching or concentration factor of 5 was used to calculate maximum stresses on a pipeline below stamukha (i.e. 20% grounded). Stamukha surveys in 2010 (Crocker et al, 2011) found that about 30 to 40 % of thermal drill locations indicated contact between the ice and the seabed. These data suggest that a concentration factor of 3 or 4 might be more representative, although the data set is as yet quite limited (and retaining the factor of 5 errs on the conservative side). A typical extreme ground pressure might be estimated using a sail height of 10m and a concentration factor or 5. This would give about 330 kPa as a ground pressure and would represent a high extreme value. As will be discussed in the next section, ice pressures may also be limited by the strength of the keels.

KEEL STRENGTH LIMIT

Keel rubble strength

The topic of the strength of ice rubble in the keels of pressure ridges was first studied in the context of pressure ridge loads on platforms (Croasdale, 1999; Palmer and Croasdale, 2012). Large scale in-situ tests were developed because it was felt that so little was understood about the formation of ice rubble and the effects of aging, that in-situ tests would give more immediate authentic data than lab tests. In-situ punch and direct shear tests were performed in Canada, Russia and the Baltic (e.g. Croasdale et al, 2001)

No targeted work has been done to measure ice rubble strength in stamukhi however some ridges tested in prior work were grounded in the landfast ice. The large scale in-situ tests give only about 40 data points (Croasdale et al, 2005). The data has an average shear strength of 12.4 kPa with a standard deviation of 6.8 kPa. The maximum shear strength measured was about 33 kPa averaged along the punch test failure planes. The data has been treated statistically and gives a 0.01 probability level value of about 38 kPa and a 0.001 probability level of about 55 kPa.

Translation of Rubble Shear Strength into a Bearing Pressure (or pseudo crushing strength)

If ice rubble is subject to load over an area, the failure pressure over the loading area can be estimated in a similar way to a footing failure in soil foundation problems. It is assumed that the shear strength of the ice is constant along the failure plane and is independent of the internal stresses prevailing in the keel due to the grounding forces. This is considered to be justified by the dominance of cohesive strength on the failure load as observed in the in-situ tests when peak loads occur.

Force normal to the ice rubble to fail the ice (F_{ice}) is given by:

$$F_{ice} = C\,K\,A \qquad (2)$$

where: C = ice keel shear strength; K = a value based on the length of the failure plane; A = contact area; and the normal pressure is given as;

$$p_f = C\,K \qquad (3)$$

In soil mechanics, footing failures will occur for values of K in the range 5 – 9 depending on the shape and depth of penetration. These values are also compatible with plasticity theory. If we use the 0.01 exceedance probability value of 38 kPa, then: p_f = 190 to 340 kPa. Combining a shear strength of 55 kPa with a K value of 9 gives an upper bound bearing pressure of about 500kPa. In the tests describes earlier, it was demonstrated that the initial failures of the cohesive bonds controlled the peak strengths and residual frictional strength was lower. For this reason, no potential effects of confinement are proposed. This is an uncertainty which warrants further investigation. However using the 55 kPa shear strength value is considered conservative enough to include any confining effects.

Assumed size effect on ice rubble strength

The largest loaded area in the punch tests from which the rubble shear strengths were derived tests was about 6m^2. Although in those tests, smaller areas were also included, it is not possible to see any size effect trend on rubble strength. Such a trend would be hard to establish from a limited data set because of the randomness in strength, as well as variations in other parameters between tests (e.g. temperature, keel depths, age of ridge).

Nevertheless, it seems very conservative to use 500 kPa over large contact areas. This is because of non-simultaneous failure and the expected brittle nature of the ice bonds between blocks. Therefore it is proposed to use the same size effect trend for ice rubble as has been established by examining large sets of ice strength data (Sanderson, 1988). This would lower the effective ice strength by area to the power - 0.5.

If we use the 500 kPa value at 6m^2, the expression for larger areas is then:

$$p_A = 500(A/6)^{-0.5} \qquad \text{for } A > 6 \qquad (4)$$

where; A is the contact area in m^2 and p_A is in kPa.

Such a size effect is speculative and further investigation is warranted.

PIT FORMATION FORCES

Given the typical sea floor pressures noted so far, it is of interest to look at their potential to create pits. Pit formation forces can be considered analogous to the surface foundation bearing capacity problem of soil mechanics, as illustrated in Figure 3. The ice rubble forming a pit is unlikely to have a flat, horizontal base like a foundation. It is more likely to have an inverted cone or pyramid shape. As a result, we can consider the ice forming the pit to be similar to the combination of the foundation and the triangular wedge that forms below the foundation when plastic failure develops. It is the surface bearing load that we consider, rather than the bearing capacity at the maximum pit depth (which would be somewhat higher.)

The bearing capacity of a surface foundation is given by the following equations (e.g. Chen and McCarron, 1991):

In clay: $$q_u = c_u N_c S_c \qquad (5)$$

In sand: $$q_u = \frac{1}{2}\gamma' B N_\gamma S_\gamma \tag{6}$$

Where, q_u = bearing stress: c_u = undrained shear strength of clay: γ' = submerged unit weight of sand: B = foundation width (or diameter): N_c, N_γ = bearing capacity coefficients (N_c = 5.14 and N_γ depends on soil friction angle ϕ, as follows: $N_\gamma = 0.1054\exp^{-0.1675\phi}$): S_c, S_γ = shape factors for shapes other than infinite strip foundation: S_c = 1.2 for square or circular foundations: S_γ = 0.6 for square or circular foundations

The purpose of the above calculations is to place limits on the pipeline loading from stamukha pits. In this respect, the ice load cases represent upper bounds in that the loads cannot be higher because the ice will fail. The soil bearing loads represent lower bounds, in the sense that if the loads were any lower the failure mechanism under discussion would not occur. We can therefore graph the load limits as shown on Figure 4 which shows the ice rubble pressure – area curve as an upper bound, and soil bearing capacities for realistic values of soil strength.

The shaded area on Figure 4 represents the potential stamukha loading in a clay with an undrained shear strength of 30 kPa. The load must be less than the ice pressure relationship, but in order for a pit to form the load must also be greater than the clay bearing capacity of 185 kPa. It is apparent that a pit larger than about 8m diameter will not form in this case, and if the ice load is less than 185 kPa a smaller pit will also not form.

Given that a pipeline will always be in a trench with backfill, either sand or clay, there are two important conclusions from Figure 4. Any pit size, including a large depression consisting of many pits under a stamukha, can potentially be formed in clay backfill. Pits in sand backfill will likely be less than 5m diameter.

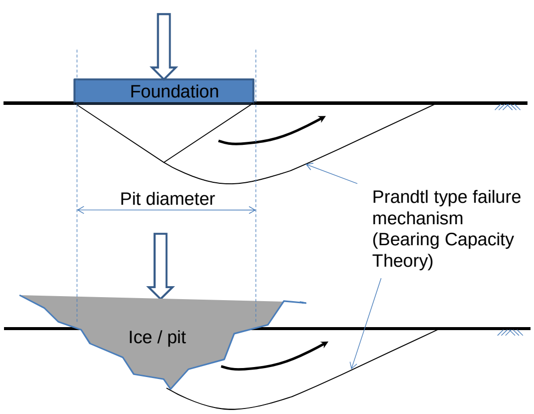

Figure 3. Surface bearing capacity problem

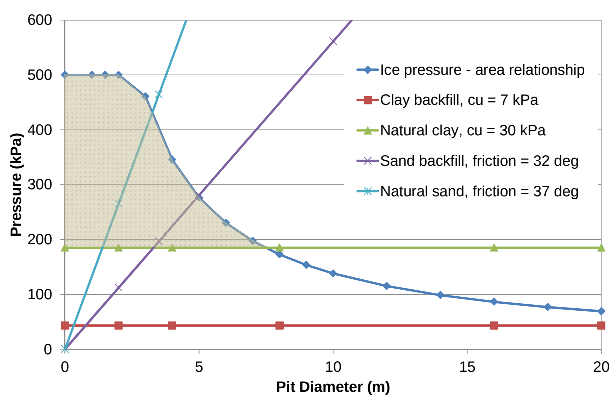

Figure 4. Ice and soil limits

The actual global loads on the pipeline from stamukha pits can now be bounded or estimated as follows: 1) If the pit depth is greater than the burial depth, consider the ice rubble pressure – area relationship for pipeline bending. In addition, local ice pressures to check denting and ovalisation may be required (beyond the scope of this paper). 2) If the pit depth is less than the burial depth, the upper bound of the soil force on the pipe can be calculated as plastic flow of the soil around the pipe which must be less than the ice force from direct contact. 3) If the pipe cannot withstand the upper bound soil force, then calculate the soil displacements from pit formation and apply those displacements to the pipe (which will result in less force than the plastic flow soil force in 2 above) (see Been et al, 2013).

OTHER ICE LOADING SCENARIOS FROM A STAMUKHA

As work proceeded into Phase 2 of the Kashagan development, additional surveys of stamukhi indicated that mechanisms during stamukha creation might lead to other loading scenarios. As well, it was recognized that weak backfill in a pipeline trench could affect the pipeline loads. Various additional loading scenarios were examined. Two of these are those originally reviewed in earlier work and just described (gravity and keel strength limit). There are two additional ice loading scenarios which might occur during stamukhi formation which have been examined; and are important because in a weak backfill could lead to direct ice contact.

Vertical Loads due to Ice Ramping Up

During the 2010 field program, detailed drilling and surveying of several stamukhi took place with the specific goal of surveying pits under stamukhi and their relationships to stamukhi geometries (Crocker et al, 2010). Several ramping-up events were noticed (e.g. Figure 5). These had also been observed in previous years. In the drilling of the stamukhi and the sea floor below, it was noted that the deepest pits (albeit only about 0.5m deep) were generally below the base of the ride up (e.g. near the "area of contact" as illustrated by pit diameter on Figure 6) and not under the highest points of the stamukha. This suggests that perhaps the forces in the ramping up process were higher than the static gravity loads and could be one of the processes leading to pits.

The process shown in Figure 6 is similar to that of ice interacting with a sloping structure, which has been the subject of much work in the context of deriving ice loads and more recently has also been adapted to quantification of ridge building forces (Croasdale, 2012).

Methods for the derivation of ice loads on sloping structures are described in the code for Arctic platforms (ISO 19906, 2010). One method is that developed by Croasdale et al (1994). It is beyond the scope of this paper to describe these models, readers are referred to the references. Typical inputs and outputs using the Croasdale method for the configuration shown in Figure 6 are shown in Table 1.

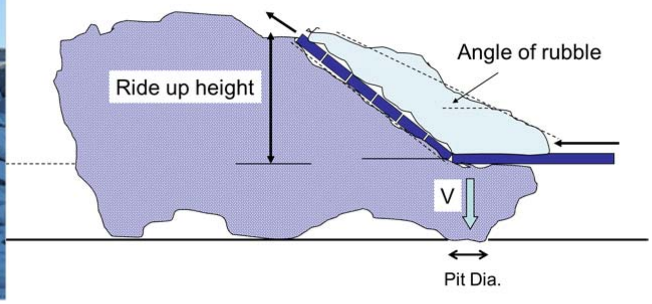

Figure 5. Ice ramps observed in 2010

Figure 6. Schematic of ice pushing into a stamukha and then ramping up

The table shows the results from a spreadsheet where pit pressures are shown for the base-case values and for a range of sensitivities. The ride up height of 15m used is considered extreme. Lower values will give significantly lower loads. The width of ice ride up was chosen as 5m. This is a judgement based on observations of ramping ice. This width must be linked to a pit size and number of pits over which the vertical force is distributed to obtain a sea floor pressure. For example we could increase the width to 10m, but if the pit size and/or number are also increased (as they should be), then the sea floor pressures would not be any greater. We feel that keeping the width to 5m in a 5m water depth and then looking at pit dimensions in the range 2.5m to 7.5m is reasonable. A pit size of 1.5m is also considered.

Table 1: Ramp-up Cases showing results for range of input parameters and pit sizes

Initial Data:	Base case	Higher strength shallow slope	High rubble str. low porosity
	A	B	C
Flexural strength of ice (kPa)	500	750	500
Specific weight of ice (kN/m^3)	8.80	8.80	8.80
Specific weight of water (kN/m^3)	10.05	10.05	10.05
Young's modulus (kPa)	5.00E+06	5.00E+06	5.00E+06
Poisson's ratio	0.3	0.3	0.3
Slope Angle (deg)	45	35	45
Rubble angle of repose (deg)	40	30	40
Rubble friction angle (deg)	0	0	0
Ride up height (m)	15	15	15
Width of ride up (m)	5	5	5
Ice slope friction	0.15	0.15	0.2
Ice-ice friction	0.15	0.15	0.2
Ice thickness (m)	0.8	0.8	0.8
Rubble porosity	0.25	0.25	0.2
Cohesion of rubble (kPa)	15	15	30
Results			
Horizontal Load (MN)	2.30	2.26	2.95
Total Vertical Load (MN)	1.69	2.35	1.95
Resultant (MN)	2.85	3.26	3.54
Vertical Pressures			
Pit Dia 1 (m)	2.5	2.5	2.5
Ground pressure 1 (kPa)	343	478	397
Pit dia 2 (m)	5	5	5
Ground pressure 2 (kPa)	86	120	99
2 pits of dia. Shown (m)	1.50	1.50	1.50
Ground pressure 2 pits (kPa)	477	664	552
3 pits 1.5m in dia. - ground press (kPa)	318	443	368

The ice thickness of 0.8m is the nominal 100 year value for ice thickness in the Caspian Sea (Verlaan and Croasdale, 2011). Most stamukhi observed are from much thinner ice. We do not see the need to go to higher thickness when combined with conservative values for ride up height.

Inspection of the results show that for the base-case and a range of assumptions on pit sizes and numbers absorbing the vertical load, the ice pressures range up to 477 kPa. The base-case is already considered conservative as it uses a ride up height of 15m and an ice thickness of 0.8m with other input values that are average or at the upper end of the range of plausible inputs. In considering some further extreme sensitivities, it is noted for single pits of 2.5m diameter, the highest value is 478 kPa. If we drop the pit diameter to 1.5m and distribute the load over two pits we get a pressure of 477 kPa for the base case but higher values (up to 664 kPa) for the some of the sensitivities. Note that the 664 kPa value is for the shallower slope ride up to 15m which will more likely be distributed over more than two pits. With three pits this case gives 443 kPa.

Overall it can be seen that this case can give ground pressures potentially higher than the simple gravity load but not significantly higher. Also note that ice rubble strength may also be a limit.

Subduction

Subduction or ride down is the opposite of ramping up and in many ways it is easier for ice to ride down than to ride up because gravity and friction forces are less in water than in air. On the other hand we have seen ice riding up on stamukhi and rubble piles but not ride down because it occurs underwater. We have seen incoming ice that reaches the edge of the rubble and then seems to disappear. It must be failing downward, but whether it ramps down to the sea floor is not known, in this work it was assumed that it does.

A range of scenarios were developed for subduction which cannot all be described in this paper. A bounding case is shown in Figure 7. In this case there is penetration of the ice rubble by the advancing ice. The ice is gradually subducted downwards to eventually interact with the sea floor. The limit in this case is assumed to be a rubbling limit force (Fe) at the point the ice enters the stamukha. The force available at the sea floor may be reduced by subtracting the frictional forces on the subducted ice from the force at the edge of the stamukha. However on further reflection these frictional forces are absorbed into the stamukha and eventually have to be reacted into the sea floor as well. In the case shown the subduction is assumed to be gradual, leading to no instabilities between blocks. In the worst case situation we will assume all the friction is transmitted to the one pit where the subducted ice contacts the sea floor – as shown in Figure 7. With this assumption, all the ice force at the ice line is transmitted to the pit area. If we assume that the pit diameter is 50% of the subducted ice width, we can calculate the sea floor pressures under these assumptions. The rationale here is that as the subducted ice penetrates further towards the sea floor, its width is eroded by say 50%. Results from this case are shown in Table 2. The values shown are assuming that the external force is limited by rubbling failure of the ice sheet (see ISO 19906, 2010 and Croasdale, 2009). Other parameters are chosen somewhat conservatively. Note that the selection of the rubbling ice load rather than crushing is based on field observations where no evidence has been seen of extensive crushing in ridge building and rubble building.

The fact that the various mechanisms for applying ice pressures to the sea floor under a stamukha all seem to converge to similar ranges of pressures and loads, and that these pressures are similar to the estimated limits for ice rubble strength, provides support to, and confidence in, the criteria selected.

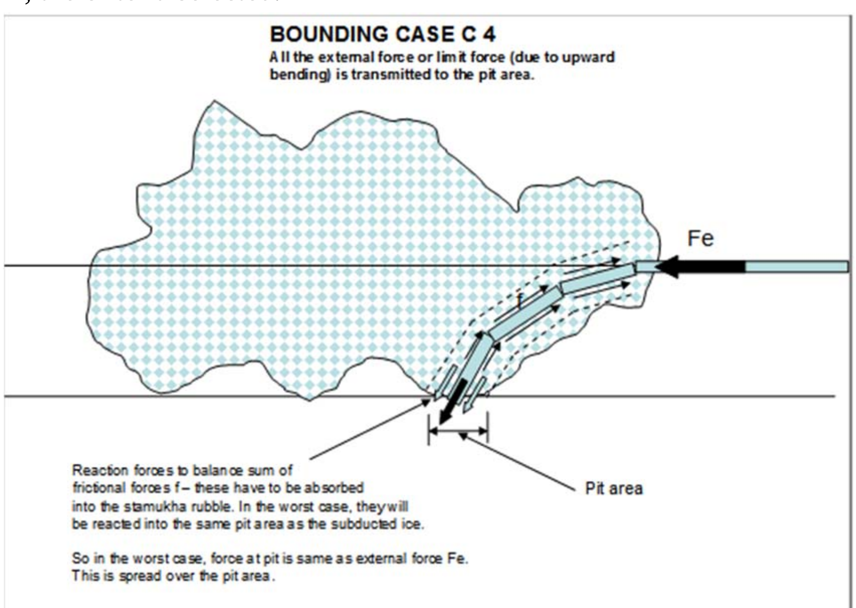

Figure 7. Internal subduction

Table 2: Subduction through interior of stamukha – limited by rubbling forces at entry point

Initial Data:	Base case	Higher R	1m ice	Smaller pit	and higher R	larger pit
	A	B	D	E	F	G
Rubbling coefficient (R) (In ISO formula)	2000	5000	2000	2000	5000	5000
Specific weight of ice (kN/m^3)	8.80	8.80	8.80	8.80	8.80	8.80
Specific weight of water (kN/m^3)	10.05	10.05	10.05	10.05	10.05	10.05
Average rubble height above subduction (m)	6.00	6.00	6.00	6.00	6.00	6.00
Horizontal penetration (m)	8.00	8.00	10.00	10.00	10.00	10.00
Water depth (m)	4	4	4	4	4	4
Width of ice subduction (m)	5	5	5	3	3	7
friction	0.15	0.15	0.15	0.15	0.15	0.15
Ice thickness (m)	0.8	0.8	1	0.8	0.8	0.8
Rubble porosity	0.25	0.25	0.25	0.25	0.25	0.25
Results:						
Length of subduction (m)	8.9	8.9	10.8	10.8	10.8	10.8
Ff (MN)	0.5	0.5	0.6	0.4	0.4	0.9
Limit ice force at A (Rubbling) (kN/m)	187	468	248	187	468	468
Ice Rubble force (MN)	0.9	2.3	1.2	0.6	1.4	3.3
Effective rubbling ice pressure (MPa)	0.2	0.6	0.2	0.2	0.6	0.6
Ice force at sea floor Fe (MN)	0.9	2.3	1.2	0.6	1.4	3.3
Pit Dia. 1 (m)	5.0	5.0	5.0	3.0	3.0	7.0
Ice pressure at sea floor (kPa)	48	119	63	80	199	85
Pit Dia 2 (m)	2.5	2.5	2.5	1.5	1.5	3.5
Ice pressure at sea floor (kPa)	191	477	252	318	795	341
Angle of force (From horizontal)	27	27	22	22	22	22

CONCLUSIONS AND RECOMMENDATIONS

In this study, we have calculated reasonable bounds on the pressures on the sea floor that can occur under stamukhi in the North Caspian Sea.

We have considered gravity loading from stationary stamukha as well as ice sheet ride up and subduction during stamukha formation. The pressures are dependent on many variables, such as stamukha height, water depth, ice sheet thickness, flexural strength, rubble shear strength, friction, and assumptions that need to be made regarding how loads are distributed through the ice rubble in a stamukha, including pit areas. Considering these variables and the bounding ice loading scenarios studied, most ice pressures calculated at the sea floor are less than about 500kPa. In some rare extreme cases, without accounting for ultimate ice rubble strength, sea floor pressures may exceed this value. However, a limiting ice pressure – area relationship for ice rubble has been suggested based on field tests which has an upper limit of 500 kPa, and is inversely proportional to the square root of the loaded area. This ice strength pressure area relationship for ice rubble will control in situations when the sea floor pressures in the scenarios considered are trending above the 500kPa value.

The forces required to fail the soil and form a pit have also been reviewed and represent a lower bound on the ice force. We calculated this soil force for a representative range of natural soils and pipeline trench backfill in the North Caspian Sea using soil mechanics bearing capacity theory. An important conclusion is that in weak backfill, the ice load scenarios can lead to direct ice contact with the pipeline in which case the pipeline loading is limited by the ice loads with an ultimate limit of the ice strength.

From the perspective of verification and due diligence, future R&D should concentrate on better understanding and quantifying ice rubble strength, its size effect and how rubble can transmit loads to soils and pipelines beneath a grounded feature (both vertically and laterally).

AKNOWLEDGEMENTS

The authors would like to thank the North Caspian Production Operations Company and the Kashagan Project partners for permission to publish the contents of this paper. We also acknowledge the tremendous contribution of many of the engineers and scientists working on the project who gave advice, collected data and helped in ways that cannot be quantified.

REFERENCES

Been, K., Croasdale, K.R., Jordaan, I. J. and Verlaan, P., 2013. Practice for Pipeline Design in Ice Scoured Environments: Application to the Kashagan Project. Proceedings of POAC 2013.

Chen, W. and McCarron, W.O. 1991. Bearing Capacity of shallow foundations. Foundation Engineering Handbook,2nd edn, H.Y Fang (ed), Chapter 4, Van Nostrand Reinhold Company, Inc, NY.

Croasdale, K.R., Cammaert, A.B., Metge, M. 1994. A Method for the Calculation of Sheet-ice Loads on Sloping Structures". IAHR Ice Symposium, Trondheim, p874-885.

Croasdale, K. R. 1999. A Study of Ice Loads due to Ridge Keels. Proc. 4th Intl. Conf. on Development of Russian Offshore (RAO), St. Petersburg.

Croasdale K.R., S. Bruneau, D. Christian, G. Crocker, J. English, M. Metge and R. Ritch. 2001. In-situ Measurements of the Strength of First-year Ice Ridge Keels. Proceedings of POAC Conference, Ottawa.

Croasdale, K. R., Comfort, G. and Been, K. 2005. Investigation of ice limits to ice gouging. Proceedings of POAC Conference. Potsdam, NY, USA.

Croasdale, K. R. 2009. Limit-force Ice Loads – An Update. Proceedings of POAC Conference, June 9-12, 2009, Luleå, Sweden.

Croasdale, K. R. 2012. Ice Rubbling and Ice Interaction with Offshore Facilities. Cold Regions Science and Technology; 76–77, 2012.

Crocker, G., Ritch, R. and Nilsen, R., 2011. Some Observations of Ice Features in the North

Caspian Sea. Proceedings of POAC 2011, Montréal, Canada.

ISO 19906:2010. Petroleum and Natural Gas Industries — Arctic Offshore Structures. International Standards Organisation, 2010.

Nilsen, R., and Verlaan, P. 2011. The North Caspian Sea Ice Conditions and how Key Ice Data is Gathered. Proceedings of POAC 2011, Montréal, Canada.

Palmer, A. C. and Croasdale K. R. 2012 Arctic Offshore Engineering. World Scientific Publishing Co. Ltd., Singapore. ,.

Sanderson, T.J.O. 1988. Ice Mechanics: Risks to Offshore Structures. Graham and Trotman, London.

Verlaan, P. and Croasdale, K., 2011. Ice Issues Relating to the Kashagan Phase II Development, North Caspian Sea. Proceedings of POAC 2011, Montréal, Canada.